
HANDBOOK OF
Intelligent Scaffolds for Tissue Engineering and Regenerative Medicine
edited by Gilson Khang

Chapter 3

PRODUCTION OF THREE-DIMENSIONAL HIERARCHICAL NANO Ti-BASED METALS SCAFFOLDS FOR BONE TISSUE GRAFTS

Shuilin Wu,[a,b] Xiangmei Liu,[a,b] Paul K. Chu,[a]* Tao Hu,[a] Kelvin W. K. Yeung,[a] Jonathan C. Y. Chung,[a] and Zushun Xu[a,b]

[a] *Department of Physics & Material Science, City University of Hong Kong, Tat Chee Avenue, Kowloon, Hong Kong*

[b] *Ministry-of-Education Key Laboratory for the Green Preparation and Application of Functional Materials, School of Materials Science and Engineering, Hubei University, Wuhan 430062, China*

*paul.chu@cityu.edu.hk

It is necessary for ideal bone implant materials to possess a hierarchical structure. This chapter describes the fabrication of three-dimensional (3D), hierarchical, porous titanium (Ti)-based metal scaffolds that fully resemble the natural structure of bones from the macro to nano scale. The fabrication process is based on the chemical reaction between the spontaneous titanium oxide layer on the exposed surface and a concentrated sodium hydroxide (NaOH) solution. A nanoskeleton layer forms on the complex surface, and subsequently one-dimensional (1D) nano titanate belts and wires directly grow on this layer. This hierarchical structure resembles the lowest level of hierarchical organization of human bone tissues. The nanostructured surface exhibits

Handbook of Intelligent Scaffolds for Tissue Engineering and Regenerative Medicine
Edited by Gilson Khang

www.panstanford.com

superhydrophilicity and favors the cell adhesion and proliferation. In addition, the *in situ* growth of nanophase materials on the scaffolds may increase the bonding strength between the nanophase materials and the scaffolds, thus minimizing the risk induced by debris shed from the surface of the nano scaffolds. The remarkable simplicity of this hydrothermal surface nano-structuring process makes it widely accessible as an enabling technique in applications of metal-based nanophase materials to bone implants.

3.1 Introduction

A normal adult has 206 bones located in different positions in the body. These bones play important roles in the normal life of human beings because they provide the basic structural support and protect important organs of the body. In addition, various physical activities are carried out by bones with the help of muscles. However, accidents can lead to traumatic or nontraumatic destruction, and there are needs for bone implants. More than 500,000 bone grafting operations are performed annually in the United States.[1,2] The supply of autografting is limited despite good clinical applications, and allografting and xenografting can easily induce pathogen transfer or rejection reactions.[3] Moreover, synthetic matrices often integrate poorly with host tissues, resulting in possible infection or other adverse body responses due to their poor corrosion, wear, and other properties.[4–6] Therefore, it is necessary to develop biocompatible bone scaffolds for bone repair or reconstruction in order to overcome the limitations of traditional therapies.[4,7–9] Before a fully biomimetic bone scaffold can be produced, it is necessary to learn the basic structures of the human bone.

Figure 3.1 shows the basic structure of bones. The cross sections of the compact bone, showing cylindrical osteons with blood vessels running along Haversian canals (in the center of each osteon), are displayed in Fig. 3.1a.

The metabolic substances can be transported by the intercommunicating systems of canaliculi, lacunae, and Volkmann's canals, which are connected with marrow cavities.[12] The various

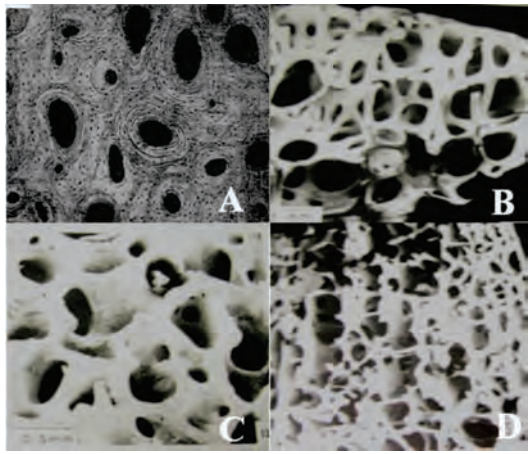

Figure 3.1. Images showing the structure of bones. (a) Optical micrograph of transverse cross section showing the microstructure of compact lamellar bone—human femora; (b) SEM image of a specimen taken from the femoral head, showing a low-density, open-cell, rodlike structure of cancellous bone; (c) SEM image of a specimen from the femoral head, showing a higher-density, roughly prismatic cell structure of cancellous bone; (d) SEM image of a specimen from the femoral condoyle, of intermediate density, showing a stress-oriented, parallel-plate structure of cancellous bone with rods normal to the plates.[10,11]

interconnecting systems are filled with body fluids, and their volume can be as high as 19%.[12] The cellular structure of cancellous bone is shown in Figs. 3.1b, 3.1c, and 3.1d.[11]

Cancellous bones are made up of an interconnected network of rods or plates. A network of rods produces low-density, open cells, whereas one of the plates gives high-density, virtually closed cells. In practice, the relative density of cancellous bones varies from 0.05 to 0.7, and technically speaking, bones with a relative density of less than 0.7 are classified as cancellous.[11]

Human bones are mainly composed of collagen (20 wt. %), hydroxyapatite mineral (69 wt. %), and water (9 wt. %).[12] Other organic materials, such as proteins, polysaccharides, and lipids, are also present in small quantities.[13] The diameter of the collagen microfibers varies from 100 to 2,000 nm, and these collagen fibers

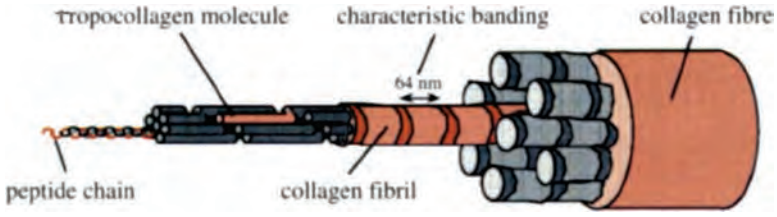

Figure 3.2. Hierarchical organization of collagen fiber.[2]

consist of carefully arranged arrays of tropocollagen molecules, which are long, rigid molecules (300 nm long and 1.5 nm wide) composed of three left-handed helices of peptides, as shown in Fig. 3.2.

Bones contain mostly type-I collagen, with some type-V collagen, and the molecules are organized into collagen fibrils formed by the assembly of tropocollagen molecules in a 3/4 staggered parallel array.[2] The typical hierarchical structure of human bones is illustrated in Fig. 3.3. Besides the hierarchical structure of collagen, the hydroxyapatite (HA) crystals present in the form of plates or needles are about 40–60 nm long, 20 nm wide, and 1.5–5 nm thick,[10–12] and the mineral phase present in the bone is not a discrete aggregation of

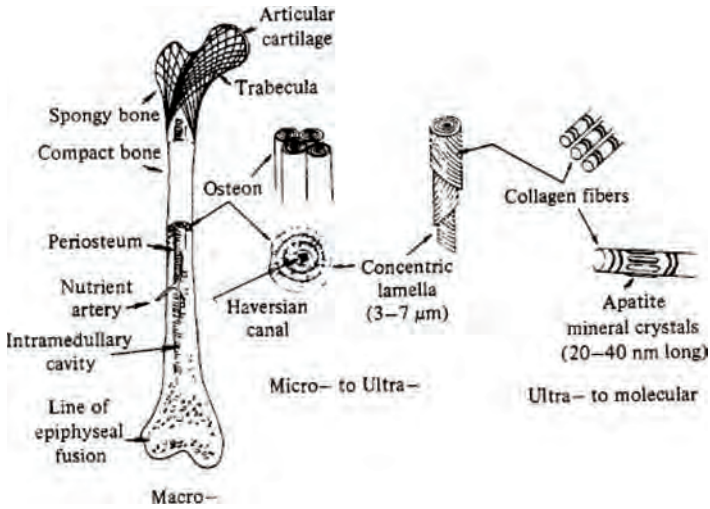

Figure 3.3. Hierarchical structures in a human long bone.[12,14]

the HA crystals but is made up of a continuous phase, evidenced by very good strength of the bone after complete removal of the organic phase.[12]

Due to this unique hierarchical structure of human bones with a macroporous structure and nano-scale organization, ideal bone implant materials must possess the hierarchical structure. This implies that the scaffolds should have not only sufficient 3D internal space and interconnective open channels that allow for mass transport, cell migration, attachment, and proliferation, as well as tissue ingrowth, but also 1D nanophase materials on the surface in order to match the lowest organization of human bones.

Because of excellent mechanical properties and biocompatibility, Ti-based biometals, such as Ti, Ti6Al4V, and nickel-titanium (NiTi), are used widely in various orthopedic applications. We have produced 3D porous NiTi and Ti scaffolds using capsule-free hot isostatic pressing (CF-HIP) powder metallurgy (PM), and the process is described here.

3.2 Fabrication and Characteristics of Macroporous Ti-Based Alloys

CF-HIP is a proven PM process to fabricate porous materials. With the use of a space holder, such as ammonia hydrogen carbonate (NH_4HCO_3), porous Ti-based metal scaffolds with adjustable porous structures, such as Ti and NiTi, have been produced successfully.[15,16] Fig. 3.4 shows the general fabrication process of Ti-based metal scaffolds using CF-HIP. In this process, metallic elemental powders including titanium are the starting materials with the ratios following the chemical compositions of the given Ti-based metals. They are mixed with a certain proportion of space holder powders (NH_4HCO_3) and pressed hydraulically under cold pressure to produce green compacts. These green compacts are preheated at 200°C to remove the space holders to acquire more initial internal pores, and these pores are filled with argon gas when the HIP unit is evacuated and backfilled with argon gas at high pressure. Afterward, these compacts are sintered at high temperatures in two steps, an initial shrinkage stage and a final expansion stage.

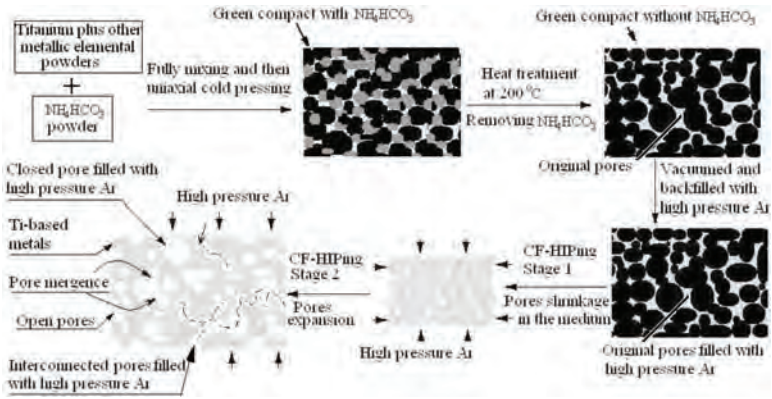

Figure 3.4. Fabrication process of macroporous Ti-based metals scaffold by CF-HIP.[15]

The typical surface morphology of the 3D macroporous Ti-based metal scaffolds is depicted in Fig. 3.5. It can be observed that most pores are interconnecting and their sizes are in the range of 50∼800 μm.

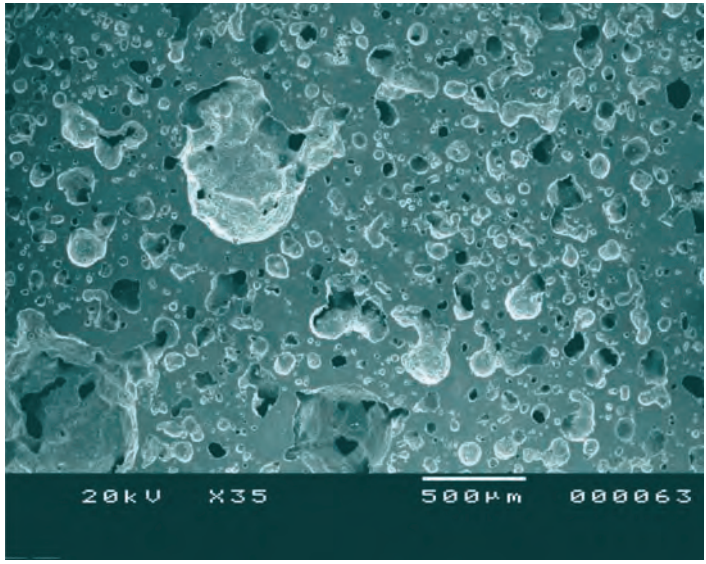

Figure 3.5. Typical porous structure of macroporous Ti-based metals by CF-HIP (NiTi).

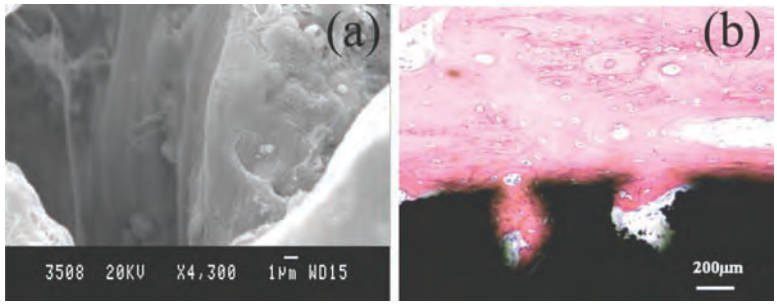

Figure 3.6. *In vitro* and *in vivo* tests of 3D macroporous Ti-based metal scaffolds produced by CF-HIP with NH_4HCO_3 as a space holder. (a) SEM image of cell in-growth on internal exposed surface of the NiTi scaffold; (b) Optical image of bone tissue (pink color) growth on the entire exposed surface of the Ti scaffold (black color).

The porosity can be controlled from 21% to 56% (in volume), and the open porosity can reach 70% using this method.[15,17]

Our previous investigations show that both 3D porous NiTi and Ti scaffolds produced by CF-HIP exhibit good mechanical properties and similar Young's modulus with human bone and that cells can attach smoothly and grow on the surface of the internal pores, as illustrated in Fig. 3.6a. After a short-term (3 months) *in vivo* test, the porous scaffolds also bode well for bone tissue in-growth, as shown in Fig. 3.6b.

3.3 Natural Growth and Characterization of 1D Nano Titanates

In view of the hierarchical organization of bones on the nano scale and the fact that nanophase materials significantly influence tissue acceptance and cell behavior[18–20] it is necessary to modify the surface of 3D macroporous Ti-based metal scaffolds to achieve a hierarchical structure on the nano scale to enhance its acceptability by nano HA crystals, tropocollagen, and other proteins from bone cells. Because of the 3D macroporous structure of Ti-based metal scaffolds, it is very difficult to treat the complex topographies using traditional line-of-sight techniques such as laser nitriding,

physical vapor deposition (PVD), and even chemical vapor deposition (CVD). Some non-line-of-sight techniques can treat almost the entire surface of the scaffolds but only induce the formation of a bioactive layer without nanophase materials.[21,22] Although the fabrication of nanostructures by layer-by-layer processing[23] pH-induced self-assembly,[24] colloidal self-assembly,[25] electron beam lithography (EBL),[20] and interference lithography (IL)[26] have been proposed, few studies have reported the natural growth of bioactive nanophase materials directly on the surface of 3D macroporous scaffolds with complex topographies.

Our recent work reveals that a lower-temperature hydrothermal treatment can induce the formation of 1D nano titanates on the entire exposed areas of 3D porous Ti-based metals such as Ti and NiTi.[16] This fabrication process of 1D nanowires/nanobelts is schematically illustrated in Fig. 3.7. The 3D porous Ti-based metal plates fabricated by CF-HIP are put in a Teflon-lined autoclave in a concentrated NaOH aqueous solution. The autoclave is heated to 60°C∼180°C for different time durations. The treated plates are washed in deionized water to remove the remaining alkaline solution and then dried at 60°C in an oven. During the heating process,

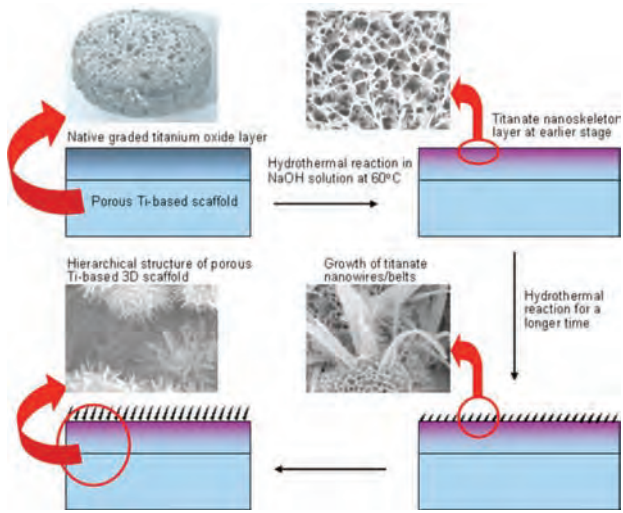

Figure 3.7. Fabrication process of 1D nanophase materials on Ti-based metals (NiTi & Ti).[16]

a titanate nanoskeleton layer forms on the exposed surface in the early stage via a reaction between native titanium oxide and NaOH.

As time elapses, some titanate nanobelts and nanowires nucleate and grow on the skeleton. Finally, a hierarchical Ti-based metal scaffold is formed. The typical surface morphology of this hierarchical structure is exhibited in Fig. 3.8. The formation of nano titanates on titanium plates and titanium dioxide powders has previously been reported, but there is still a dispute on the phase composition of these nano titanates. Peng and Chen[27] ascribe the formation of titanates to the direct reaction between Ti and the NaOH aqueous solution when the Ti plate is immersed in a concentrated alkaline solution. The reaction is shown in the following equation:[27]

$$6Ti + 2NaOH + 11H_2O \rightarrow Na_2Ti_6O_{13} + 12H_2(g) \qquad (3.1)$$

When the starting material is titanium dioxide, Sun *et al*. attribute the formation of nano titanates to the following hydrothermal reaction:[28]

$$4TiO_2 + 2NaOH \rightarrow Na_2Ti_4O_9 + H_2O \qquad (3.2)$$

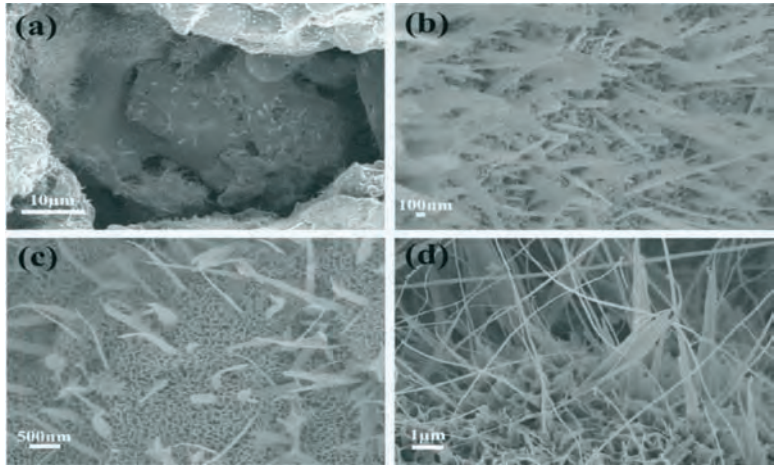

Figure 3.8. Morphologies of a hydrothermally treated 3D porous NiTi scaffold. (a) Typical surface morphology of an exposed internal pore after treatment at 60°C for 240 hours; (b) Morphology of the wall of the exposed pore in (a); (c) Morphology of the bottom of the pore in (a); (d) General growth condition of nanowires/nanobelts on the exposed surface after treatment at 60°C for 240 hours.[16]

Using the same starting materials and the same process, Yang *et al.*[29] have obtained nano titanates composed of $Na_2Ti_2O_4(OH)_2$ using the following hydrothermal reaction:

$$2TiO_2 + 2NaOH \rightarrow Na_2Ti_2O_4(OH)_2 \quad (3.3)$$

Robert Armstrong proposes that hydrothermally synthesized nano titanates are sodium hydrogen titanates with a general formula of $Na_yH_{2-y}Ti_nO_{2n+1} \cdot xH_2O$.[30] Our results confirm that these 1D nano titanates produced by the reaction between the matrix scaffold and the concentrated alkaline solution are composed of a predominant phase of $Na_2Ti_2O_5 \cdot H_2O$ and traces of other phases.[16] In the case of porous Ti-based scaffolds produced by PM, the hydrothermal reaction mechanism is more complex because the metallic Ti and surface native titanium dioxides may react with the concentrated alkaline solution. In addition, our investigation discloses that these 1D nanowires/nanobelts grown on the scaffold are unstable under high-energy electron impact.[16] As shown in the TEM picture in Fig. 3.9, the length of these 1D nanobelts on the surface can reach 10 μm.

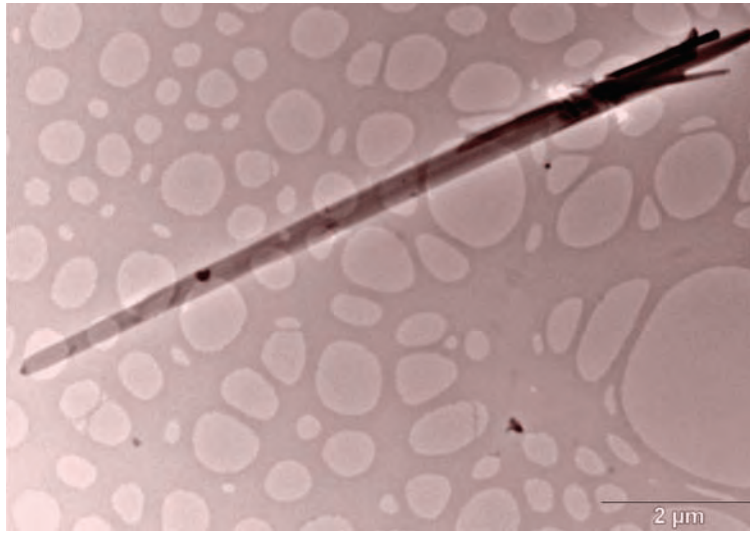

Figure 3.9. TEM image of single 1D nanobelt of titanate scratched from the hydrothermal-treated Ti-based metal scaffold.

From the perspective of surface modification of 3D porous scaffolds, the biggest advantage of this hydrothermal process is that the alkaline solution can reach the entire exposed surface, irrespective of the complex topography, due to its non-line-of-sight nature. In contrary, most other reported techniques can only be used to fabricate nano/micro porous structures on planar samples with simple topographies.[20,31–33] Furthermore, this hierarchical scaffold has no distinct interface between the substrate and the nanostructured layer, which is different from hybrid composites filled with a layer of organic nano matrix by self-assembly.[34] The natural growth directly from the substrate strengthens the bonding between the scaffolds and nanowires/nanobelts, favoring a smooth junction between bone tissues and scaffolds, benefiting the long-term fixation of the 3D scaffolds, which can possibly extend the lifetime of the implants. Our recent contact-angle measurements indicate that 1D surface nano titanates can significantly improve the hydrophilicity of both Ti and NiTi scaffolds.[16] On the other hand, other biodegradable polymer scaffolds, such as poly(L-lactic acid) (PLLA),[19,35] poly(DL-lactic-*co*-glycolic acid) (PLGA),[35] polystyrene (PS),[36] and poly(ethylene terephthalate) (PET),[37] have to undergo surface modification before *in vitro* or *in vivo* tests due to their hydrophobic nature. In practice, good hydrophilicity can improve the biocompatibility of biomaterials. Our cell culture tests show that these surface 1D titanates nanowires/nanobelts significantly enhance cell adhesion and proliferation (Fig. 3.10).

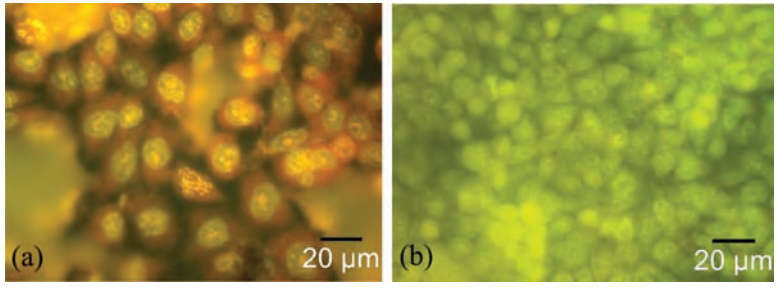

Figure 3.10. Microscopic view of cell growth on the surface of microporous NiTi with or without nanostructured titanate. (a) Untreated surface and (b) surface with nanostructured titanate.[16]

This is because the surface nanophase materials increase the active points where cells and proteins can accept and attach, besides the good hydrophilicity.

3.4 Conclusions and Outlook

This chapter focuses on the fabrication of a biomimetic Ti-based metal scaffold to highly resemble the hierarchical structure of human bones on both the macro and nano scales. A new PM method, CF-HIP, with a removable space holder, is utilized to fabricate 3D macroporous Ti-based metal scaffolds with adjustable porous structures. Cell culture results show that these metal scaffolds produced by CF-HIP have good cytocompatibility and are suitable for cell in-growth. Short-term *in vivo* implantation indicates that this macroporous structure of Ti-based metal scaffolds favors bone tissue in-growth. A facile hydrothermal process is effective in treating the entire exposed surface of the scaffolds due to its non-line-of-sight nature. Furthermore, the hydrothermal reaction between the Ti-based metal scaffolds and a concentrated alkaline solution can easily induce the formation of 1D titanate nanowires/nanobelts on the exposed surface, mimicking the hierarchical organization of human bones on the lowest level. These hydrophilic 1D titanate nanowires/nanobelts favor cell attachment and proliferation. Before the clinical application of these nano Ti-based metal scaffolds, two key problems must be solved. The first one is how to precisely control the growth direction, nano size, and nano shape. The second one is to understand the interfacial structure so as to control the bonding strength between the surface 1D nanophase materials and Ti-based metal scaffolds to avoid debris shed from the nanophase materials. It is also essential to carry out pertinent *in vivo* animal evaluations to investigate the effects of these nanophase materials on the growth of bone tissues.

Acknowledgments

This work was supported by the Hong Kong Research Grants Council (RGC) General Research Funds (GRF), Grant nos. City U

112306 and 112307; the National Natural Science Foundation of China Grant no. 50901032; the Ministry of Education Specialized Research Fund for the Doctoral Program of Universities Grant no. 20094208120003; the Hubei Provincial Natural Science Foundation Grant no. 2009CBD359; and the Hubei Provincial Middle-Young Research Fund Grant no Q20101010.

References

1. S. N. Parikh, *Orthopedics*, **1301** (2002).
2. K. A. Hing, *Phil. Trans. R. Soc. Lond.* **A362**, 2821 (2004).
3. R. Murugan and S. Ramakrishna, *Tissue Eng.*, **1845** (2007).
4. S. J. Hollister, *Nat. Mater.* **4**, 518 (2005).
5. A. P. Sclafani, J. R.Thomas, A. J. Cox, and M. H. Cooper, *Arch. Otolaryngol. Head Neck Surg.*, **328** (1997).
6. G. Chen, T. Ushida, and T. Tateishi, *Macromol. Biosci.*, **67** (2002).
7. F. T. Moutos, L. E. Freed, and F. Guilak, *Nat. Mater.* **162** (2007).
8. V. S. Lin, M. C. Lee, S. O'Neal, J. McKean, and K. L. P. Sung, *Tissue Eng.* **443** (1999).
9. J. L. Drury and D. J. Mooney, *Biomaterials*, **4337** (2003).
10. J. L. Katz, In *Symposia of the Society for Experimental Biology, Number XXXIV: The Mechanical Properties of Biological Materials* (Cambridge University Press, 1980), p. 99.
11. L. J. Gibson and M. F. Ashby, Eds., *Cellular Solids* (Cambridge Press, Cambridge, 1997).
12. J. B. Park, *Biomaterials Science and Engineering* (Plenum Press, NY, 1987).
13. S.L. Gunderson and R. C. Schiavone, In Ed. S. M. Lee, *International Encyclopedia of Composites* (VCH Publishers, NY, 1991), p. 324.
14. W. Suchanek and M. Yoshimura, *J. Mater. Res.*, **94** (1998).
15. S. L. Wu, C. Y. Chung, X. M. Liu, P. K. Chu, J. P. Y. Ho, C. L. Chu, Y. L. Chan, K. W. K. Yeung, W. W. Lu, K. M. C. Cheung, and K. D. K. Luk, *Acta Mater.*, **3437** (2007).
16. S. L. Wu, X. M. Liu, T. Hu, P. K. Chu, J. P. Y. Ho, Y. L. Chan, K. W. K. Yeung, C. L. Chu, and T. F. Hung, *Nano Lett.*, **3803** (2008).
17. S. L. Wu, X. M. Liu, Y. L. Chan, C. Y. Chung, P. K. Chu, C. L. Chu, K. O. Lam, K. W. K. Yeung, W. W. Lu, and K. D. K. Luk, *Surf. Coat. Technol.*, **2458** (2008).

18. A. S. Andersson, J. Brink, U. Lidberg, and D. S. Sutherland, *IEEE Trans. Nanobiosci*., **49** (2003).
19. K. M. Woo, J. H. Jun, V. J. Chen, J. Y. Seo, J. H. Baek, H. M. Ryoo, G. S. Kim, M. J. Somerman, and P. X. Ma, *Biomaterials*, **335** (2007).
20. M. J. Dalby, N. Gadegaard, R. Tare, A. Andar, M. O. Riehle, P. Herzyk, C. D. W. Wilkinson, and R. O. C. Oreffo, *Nat. Mater*., **997** (2007).
21. S. L. Wu, P. K. Chu, X. M. Liu, C. Y. Chung, J. P. Y. Ho, C. L. Chu, S. C. Tjong, K. W. K. Yeung, W. W. Lu, and K. M. C. Cheung, *J. Biomed. Mater. Res*., **A79**, 139 (2006).
22. S. L. Wu, X. M. Liu, Y. L. Chan, J. P. Y. Ho, C. Y. Chung, P. K. Chu, C. L. Chu, K. W. K. Yeung, W. W. Lu, and K. M. C. Cheung, *J. Biomed. Mater. Res*., **A81**, 948 (2007).
23. E. Jan and N. A. Kotov, *Nano Lett*., **1123** (2007).
24. J. D. Hartgerink, E. Beniash, and S. I. Stupp, *Science*, **1684** (2001).
25. C. Huwiler, T. P. Kunzler, M. Textor, J. Voros, and N. D. Spencer, *Langmuir*, **5929** (2007).
26. J. H. Jang, C. K. Ullal, T. Gorishnyy, V. V. Tsukruk, and E. L. Thomas, *Nano Lett*., **740** (2006).
27. X. Peng and A. Chen, *Adv. Funct. Mater*., **1355** (2006).
28. X. Sun, X. Chen, and Y. Li, *Inorg. Chem*., **4996** (2002).
29. J. Yang, Z. Jin, X. Wang, W. Li, J. Zhang, S. Zhang, X. Guo, and Z. Zhang, *Dalton Trans*., **3898** (2003).
30. A. R. Armstrong, G. Armstrong, J. Canales, and P. G. Bruce, *Angew. Chem.-Int. Edit*., **2286** (2004).
31. J. Y. Lim and H. J. Donahue, *Tissue Eng*., **1879** (2007).
32. M. Karlsson and L. Tang, *J. Mater. Sci: Mater. Med*., **1101** (2006).
33. W. Sun, J. E. Puzas, T. J.Sheu, X. Liu, and P. M. Fauchet, *Adv. Mater*., **19** (921).
34. T. D. Sargeant, M. O. Guler, S. M Oppenheimer; A Mata, R. L. Satcher, D. C. Dunand, and S. I. Stupp, *Biomaterials*, **161** (2008).
35. A. G. Mikos, M. D. Lyman, L. E. Freed, and R. Langer, *Biomaterials*, **55** (1994).
36. J. A. Neff, K. D. Caldwell, and P. A. Tresco, *J. Biomed. Mater. Res*., **511** (1998).
37. M.Yamamoto, K. Kato, and Y. Ikada, *J. Biomed. Mater. Res*., **29** (1997).